Available online at www.sciencedirect.com
SCIENCE DIRECT®
C. R. Palevol 4 (2005) 473–486
COMPTES RENDUS PALEVOL
http://france.elsevier.com/direct/PALEVO/

General Paleontology (Paleoecology)

Summary of Early Triassic carbon isotope records

Frank A. Corsetti [a,*], Aymon Baud [b], Pedro J. Marenco [a], Sylvain Richoz [c]

[a] *Department of Earth Sciences, University of Southern California, Los Angeles, CA 90089–0740, USA*
[b] *Parc de la Rouvraie 28, CH-1018 Lausanne, Suisse*
[c] *Geological Museum, UNIL-BFSH2, CH-1015 Lausanne, Suisse*

Received 2 November 2004; accepted 18 May 2005

Available online 08 August 2005

Written on invitation of the Editorial Board

Abstract

Much attention has been given to the negative $\delta^{13}C$ anomaly nearly coincident with the Permian–Triassic boundary. New data indicate a stepwise decline in $\delta^{13}C$ initiating before the Latest Permian extinction event followed by highly variable $\delta^{13}C$ values during the remaining Early Triassic. $\delta^{13}C$ values appear much less erratic as global metazoan diversity increased in the Middle Triassic. Given the previously unappreciated magnitude of isotopic change and the number of large $\delta^{13}C$ excursions that occurred during the Early Triassic, catastrophic mechanisms like methane release/bolide impact become less attractive to explain the Early Triassic carbon isotopic record as a whole. ***To cite this article: F.A. Corsetti et al., C. R. Palevol 4 (2005)***.

Résumé

Synthèse des valeurs isotopiques du carbone au Trias inférieur. Un intérêt soutenu a été porté à l'anomalie isotopique du carbone, qui coïncide apparemment avec la limite Permien–Trias. De nouveaux travaux montrent que la chute des valeurs isotopiques est en escalier et débute avant l'extinction en masse fini-permienne ; ils prouvent aussi l'existence de variations extrêmes de celles-ci durant le Trias inférieur, et ceci jusqu'à l'Anisien précoce. Par la suite, en même temps que la diversité augmente, ces valeurs apparaissent beaucoup plus stables. Au vu de la magnitude des variations isotopiques et des excursions de grande ampleur au Trias inférieur, les explications « catastrophistes » de relâchement massif de méthane ou d'impact sont devenues moins attractives, sans cependant pouvoir être ignorées. ***Pour citer cet article : F.A. Corsetti et al., C. R. Palevol 4 (2005)***.

Keywords: Permian–Triassic boundary; Negative $\delta^{13}C$ anomaly; Carbon isotopic record

Mots clés : Limite Permien–Trias ; Anomalie négative du $\delta^{13}C$; Enregistrement isotopique du carbone

* Corresponding author.
E-mail address: fcorsett@usc.edu (F.A. Corsetti).

1631-0683/$ - see front matter © 2005 Académie des sciences. Published by Elsevier SAS. All rights reserved.
doi:10.1016/j.crpv.2005.06.004

1. Introduction

The most devastating mass extinction in the Phanerozoic occurred at the end of the Permian when over 80% of all marine species went extinct [25,83,93]. While the Permo-Triassic boundary has been the focus of much attention, a growing body of evidence demonstrates that the *entire* Early Triassic is unusual from the paleobiological, sedimentological, and geochemical point of view (see other papers in this volume). Biotic diversity did not begin to recover to pre-extinction levels until the Middle Triassic, approximately 4 to 6 Myr later [71,75]. In contrast, the Cretaceous–Tertiary recovery interval lasted less than 1 Mayr, and less than ~100 000 years for many taxa [37]. The Early Triassic is also characterized by a conspicuous metazoan reef gap, a "chert gap" in tropical and northern hemisphere domains (suggesting the near extinction of radiolaria possibly associated with the collapse of thermohaline circulation), and a "coal gap," suggesting the termination of peat-forming floras [8,24,27,37,85,86].

Unusual sedimentary facies are also found in anomalous volume during the Early Triassic, including large seafloor fans (pseudomorphs of aragonite), voluminous flat pebble conglomerates, and the proliferation of microbial facies [7,81].

A variety of recent studies conclude that propagated environmental stresses were present throughout most of the Early Triassic and helped to shape the protracted nature of the biotic recovery (e.g., [24,35–37,104]). However, many of the hypotheses formulated to explain the extinction are geologically 'instantaneous' (e.g., massive methane release, bolide impact, etc. [9,61]) and would not likely explain the existence of potentially deleterious conditions for millions of years. Others, such as those related to anoxic oceanic conditions and poor circulation [45,72,99,101] are more appealing in the long term, but have been recently questioned [10,109]. Thus, the jury is still out on the cause/causes of the mass extinction and the delayed recovery interval – a good summary is provided by [24,25].

Here, we review the available carbon isotopic data from around the world and demonstrate that the exogenic carbon cycle remained perturbed throughout Early Triassic time and that the 'boundary excursion' simply marks the onset of 4 to 6 Myr of unusual ocean chemistry. We will review the $\delta^{13}C$ record for marine strata with respect to the boundary interval, for which there is a relatively large amount of data. Our main purpose, however, is to examine the $\delta^{13}C$ record for the duration of the Early Triassic. The few studies that provide $\delta^{13}C$ data beyond the boundary interval (most notably [1,2,5,44,80,88]) reveal unusually large negative and positive excursions in the extinction aftermath that indicate changes in biogeochemical cycling of carbon not seen since Cambrian and earlier times.

2. Late Permian–Early Triassic carbon isotopic records

Most of the published carbon isotope studies center on the Permian–Triassic boundary (e.g., [4,5,16,18,22,25,30,38,39,42,43,62,65,78,91]) and rarely sample strata beyond the Griesbachian (the first stage of the Early Triassic). The location of these studies is plotted on Fig. 1 and Table 1 provides a list of known localities with isotopic data. The presence of the supercontinent Pangaea controlled the position of the four main oceans of the time, the Panthalassic Ocean, the Paleotethys Ocean, the Neotethys Ocean and the Boreal Ocean (Fig. 1). As the name would imply, the vast Panthalassic Ocean spanned most of the globe, but few carbon isotope studies sample Panthalassic stratigraphic sections. The smaller Neotethys Ocean, characterized by abundant isolated platforms and carbonate shelves, was predominantly equatorial. Strata deposited in the northerly Boreal Ocean, the smallest of the Early Triassic oceans, are predominantly siliciclastic. As such, most of the limited amount of carbon isotopic data from the Boreal realm originates from organic matter rather than carbonate. We will present a summary of the $\delta^{13}C$ data from the Permo-Triassic boundary and then focus on the post-boundary Early Triassic record.

2.1. Carbonate versus organic carbon isotopic signatures

It is generally assumed that the $\delta^{13}C$ of carbonate ultimately reflects the carbon isotopic composition of the dissolved HCO_3^{2-} in the water mass from which the carbonate precipitated. However, where carbonates are rare or absent, some have substituted the $\delta^{13}C$ of bulk organic matter and assumed a fractionation factor, usually ~25 to 28‰ (reflecting the isotopic offset imparted by photosynthetic phytoplankton common in

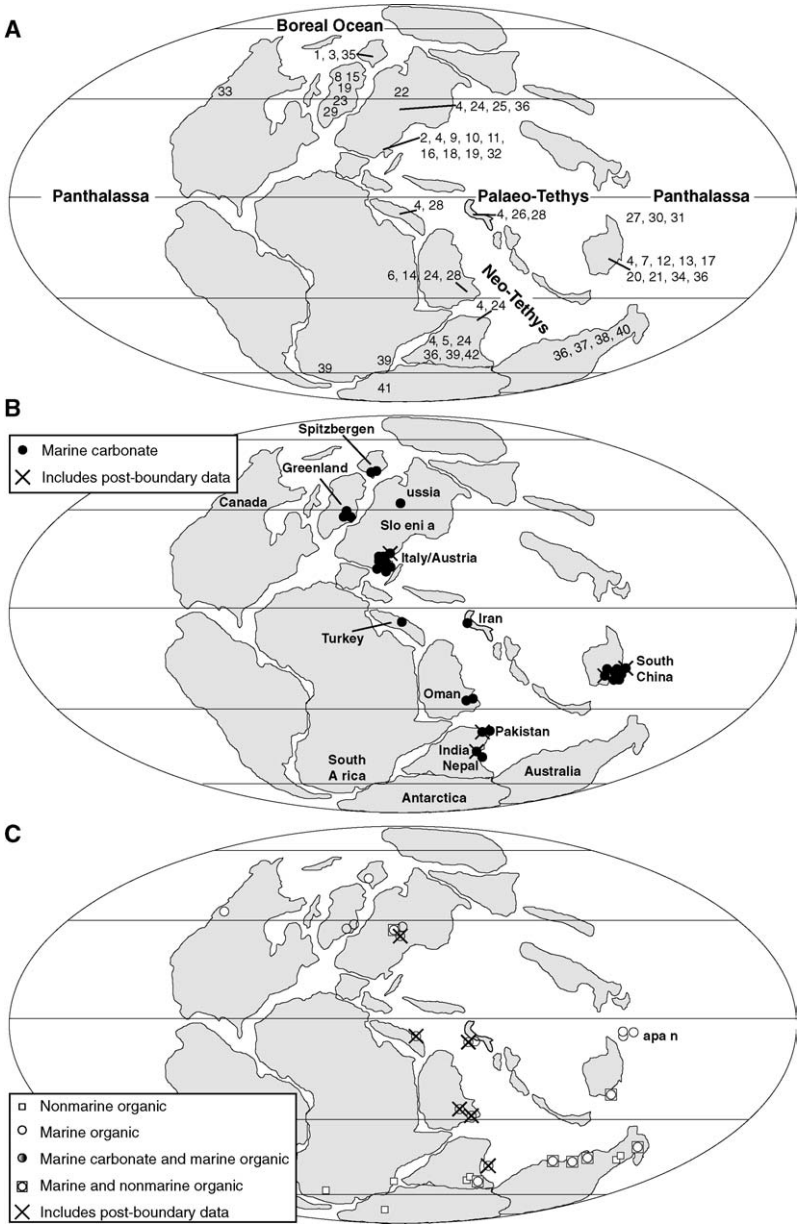

Fig. 1. Paleogeographic reconstruction during the Permo-Triassic transition (highly modified from [24]). Accreted terranes in Japan are from Panthalassa, but the original locations are uncertain. (**A**) Location of key sections given in Table 1 and major oceans. Position of numbers are near, but not necessarily upon, the locality in question. (**B**) Localities with δ^{13}C of marine carbonate. The present-day continental segments are denoted for reference. Note the concentration of carbon isotope studies around the Neotethys versus other regions. (**C**) Localities with δ^{13}C of other phases (organic and/or non-marine).

Fig. 1. Reconstitution de la paléogéographie de la transition Permien–Trias (légèrement modifiée d'après 24). Les domaines du Japon résultant d'accrétions appartiennent à la Panthalassa, mais leur localisation originelle demeure incertaine. (**A**) Localisation des affleurements clés figurant sur le Tableau 1 ainsi que des principaux océans. Les chiffres sont situés à proximité, mais pas obligatoirement à l'emplacement exact, des localités concernées. (**B**) Localités avec des valeurs du δ^{13}C mesurées dans des carbonates marins. Le contour des continentaux actuels et le nom des pays sont indiqués à titre de repères. Noter la concentration des études portant sur les isotopes du carbone autour de la Téthys par rapport à d'autres régions. (**C**) Localités avec des valeurs du δ^{13}C mesurées dans d'autres faciès (organique ou/et non marin).

Table 1
A non-exhaustive list of carbon isotope studies across the Permo-Triassic boundary. Only the first publication by any given research group is listed unless new data was provided by the same group in subsequent publications. References in boldface include post-Griesbachian isotopic profiles. References with * are reported in conference proceedings or other literature
Tableau 1. Liste non exhaustive des études portant sur les isotopes du carbone du passage Permien–Trias. Seule la première publication des équipes de recherche a été mentionnée, sauf si des données nouvelles ont été ajoutées dans des publications plus récentes. Les références en caractères gras incluent des profils isotopiques postérieurs au Griesbachien. Les références avec astérisques proviennent de comptes rendus de congrès ou d'autres travaux.

Reference	**Carbon phase**	**Location (see** Fig. 1)
Gruszczynski et al., 1989 [33]	Brachiopod calcite	1. Spitzbergen
Korte, 1999 [58]	**Brachiopod calcite**	**2. Italy**
Malkowski et al., 1989 [66]	Brachiopod calcite	3. Spitzbergen
Baud et al., 1989 [4]	Marine carbonate	4. Slovenia, Greece Turkey, Armenia, Iran, Pakistan, India, China
Baud et al., 1996 [5]	**Marine carbonate**	**5. Indian Subcontinent**
Baud et al., 1999 [6]*	Marine carbonate	6. Oman
Chen et al., 1984 [16]	Marine carbonate	7. China
Clemmensen et al., 1985 [17]	Marine carbonate	8. Greenland
Holser and Magaritz, 1985 [40]	Marine carbonate	9. Austria
Holser et al., 1989 [42]	Marine carbonate	10. Austria
Horacek et al., 2000 [44]*	**Marine carbonate**	**11. Italy**
Jin et al., 2000 [50]	Marine carbonate	12. China
Krull et al., 2004 [62]	Marine carbonate	13. China
Krystyn et al., 2003 [63]	Marine carbonate	14. Oman
Magaritz, 1989 [64]	Marine carbonate	15. Greenland
Magaritz et al., 1988 [65]	Marine carbonate	16. Italy
Nan et al., 1998 [77]	**Marine carbonate**	**17. China**
Newton et al., 2004 [78]	Marine carbonate	18. Italy
Oberhansli et al., 1989 [79]	Marine carbonate	19. Greenland, Italy
Payne et al., 2004 [80]	**Marine carbonate**	**20. China**
Xu and Yan, 1993 [106]	Marine carbonate	21. China
Zakharov et al., 1999 [108]	Marine carbonate	22. Russia
Stemmerik and Piasezki, 1997 [94]	Marine carbonate and organic	23. Greenland
Atudorei, 1999 [1]*	**Marine carbonate and organic**	**24 Romania, Albania, India, Pakistan, Nepal, Oman**
Dolenec et al., 1998; 1999 [20,21]	Marine carbonate and organic	25. Slovenia
Heydari et al., 2000; Korte et al., 2004 [39,60]	Marine carbonate and organic	26. Iran
Musashi et al., 2001 [76]	Marine carbonate and organic	27. Japan
Richoz, 2004 [88]*	**Marine carbonate and organic**	**28 Turkey,** Iran, **Oman**
Twitchett et al., 2001 [95]	Marine carbonate and organic	29. Greenland
Ishiga et al., 1993 [46]	Marine organic	30. Japan
Retallack et al., 1997 [87]	Marine organic	31. Japan
Sephton et al., 2002 [91]	Marine organic	32. Italy
Wang et al., 1994 [97]	Marine organic	33. Canada
Wang et al., 1996 [98]	Marine organic	34. China
Wignall et al., 1998 [102]	Marine organic	35. Spitzbergen

(continued on next page)

Table 1
(continued)

Reference	Carbon phase	Location (see Fig. 1)
Hansen et al., 2000 [38]	Marine and nonmarine organic	36. Slovenia, India, China, Australia
Morante 1994, 1996 [73,74]	Marine and nonmarine organic	37. Australia
Buick et al., 2002 [15]*	Nonmarine organic	38. Australia
de Wit et al., 2002 [18]	Nonmarine organic	39. India, Madagascar, South Africa
Foster et al., 1997, 1999 [28,29]*	Nonmarine organic	40. Australia
Krull et al., 2000 [61]	Nonmarine organic	41. Antarctica
Sarkar et al., 2003 [89]	Nonmarine organic	42. India

marine environments), to compare with $\delta^{13}C$ variations in carbonate-rich sections. This approach works well for open ocean settings far from the influence of continents and for geologically older sections that were deposited before the advent of a volumetrically significant terrestrial biomass (e.g., Precambrian). Unfortunately, Permo-Triassic sections that were deposited near continents may contain a mix of terrestrial and marine organic carbon (e.g., [29,32,90]). Terrestrial and marine carbon may have vastly different $\delta^{13}C$ compositions and the mixing of the two may result in an averaged $\delta^{13}C$ value for bulk carbon that does not directly reflect the CO_2 fixed by photoautotrophs in the marine environment. Thus, the $\delta^{13}C$ of bulk organic carbon where continental influence may be present cannot be confidently interpreted to reflect whole ocean shifts in $\delta^{13}C$ without intensive compound specific isotopic studies. For example, Foster et al. [28] demonstrated that a negative $\delta^{13}C_{organic}$ excursion in the marine Woodada-2 borehole, Australia, was caused by the switch from a preponderance of isotopically heavy reworked woody material in the Latest Permian to isotopically lighter acritarch-dominated material in the Early Triassic and not by a change in the $\delta^{13}C$ of marine CO_2. Therefore, the $\delta^{13}C$ profiles generated from organic matter alone are considered less robust than those from unaltered carbonates and correlations based solely on shifts in bulk organic carbon should be treated with caution.

2.2. Permo-Triassic Boundary $\delta^{13}C$ record

In general, the Permo-Triassic transition is characterized by a stratigraphically sharp negative $\delta^{13}C$ excursion from a Latest Permian peak of ~+2 to +4‰ to an isotopic nadir of ~ –1‰ (Fig. 2). The stratigraphic position of the $\delta^{13}C$ excursion varies from study to study, although some of this confusion may stem from the fact that the GSSP for the basal Triassic was only recently approved and now coincides with the first occurrence of the conodont *H. parvus* [107]. Currently, most workers place the isotopic nadir within the Latest Permian, in association with the Latest Permian Changxingian extinction event. The excursion precedes the base of the Triassic at the type section in Meishan [50]. Another good example of this would be the Dajiang section in South China [80]. Here, the base of the Triassic, coincident with the first occurrence of *H. parvus,* occurs tens of meters above the isotopic nadir, where $\delta^{13}C$ values are relatively constant at ~+2‰. According to the new data of Richoz [88], the C isotope shift appears stepwise: the first shift occurred in the Late Changxingian before the mass extinction and the second shift follows the mass extinction (but precedes the first occurrence of of *H. parvus*).

In some sections, the stratigraphic duration of the negative anomaly spans many tens of meters. In the Gartnerkofel core (Austria), for example, the $\delta^{13}C$ anomaly spans approximately 30 m; in detail, the profile declines from ~+3‰ to +1‰ over the first ~25 m and then declines more abruptly to ~–1‰ over ~5 m [43]. An examination of the literature would suggest that most workers consider the abrupt decline to represent the characteristic "negative excursion" associated with the boundary transition. As stated above, the decline does not appear as abrupt in some sections; instead, it appears stepwise and spans at least two conodont subzones [88]. On the South China Platform [80], the anomaly spans 50 m at the Dajiang section, from +4‰ to ~–1‰, with an increase in the rate of isotopic change in the last 5 meters. At the Guryul section in Kashmir [1,5], the anomaly spans ~30 m from +2‰ to –4‰, without an oversteepening of the trend in the

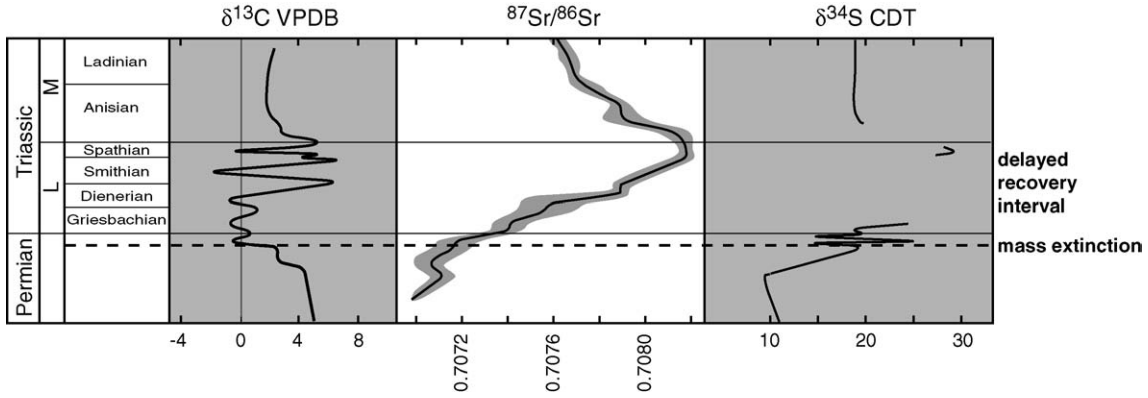

Fig. 2. Compilation of important isotopic events in the Early Triassic. Note that the $\delta^{13}C$ record is extraordinarily oscillitory and that the boundary excursion is but one of several large $\delta^{13}C$ excursions. $\delta^{13}C$ data originate primarily from [1,5,80,88], $^{87}Sr/^{86}Sr$ data originate from [58,70], and $\delta^{34}S$ data originate from [42,54,67,68,78].

Fig. 2. Compilation des événements isotopiques significatifs du début du Trias. Noter que les valeurs du $\delta^{13}C$ varient énormément et que l'excursion qui a lieu à la limite Permien–Trias ne représente qu'une excursion parmi d'autres tout aussi importantes. Les valeurs du $\delta^{13}C$ proviennent initialement des données de [1,5,80,88], les valeurs du $^{87}Sr/^{86}Sr$ de [58,70], et celles du $\delta^{34}S$ de [42,54,67,68,78].

upper part of the section. Such discrepancies likely originate from stratigraphic completeness and sampling issues (cf. [69]).

The temporal duration of the anomaly is also debated [13,65,75,82]. If we take a simplistic approach and compare the stratigraphic duration of the anomaly versus average sedimentation rate for carbonate platformal sections for these examples (17–200 m/Ma) (e.g., [11]), the decline from positive $\delta^{13}C$ values in the Latest Permian to the isotopic nadir would appear to last ~1 Myr, with the most rapid decrease encompassing the last 160 000 years. Bowring et al. [13] studied the geochronology of the type section at Meishan and determined that the $\delta^{13}C$ excursion lasted less than 165 000 years, in good agreement with the average sedimentation rate model. Alternatively, Rampino et al. [82] employed astronomically tuned cyclostratigraphy of the Gartnerkofel core to suggest a much shorter duration, less than 30 000 years. More recently, Mundil et al. [75] recalibrated the Permo-Triassic boundary interval using different geochronologic methods than Bowring et al. [13] in South China and suggest that the negative anomaly may have lasted as long as 2 Myr, given the uncertainties in their data. It is critical to know the duration of the anomaly: shorter durations favor catastrophic processes while longer durations preclude such processes. Thus, the uncertainty surrounding its duration hampers our ability to constrain the cause of the negative anomaly.

2.3. Early Triassic $\delta^{13}C$ record

The extreme magnitude of the end-Permian extinctions attracts much attention, such that the $\delta^{13}C$ record for the remaining Early Triassic has been virtually ignored and the available data originate from only a few sections (see Fig. 1 and Table 1). Indeed, few studies report useful $\delta^{13}C$ profiles beyond a few tens of meters of the base of the Triassic. Baud et al. [5] were the first to use systematically sampled complete sections spanning the Lower Triassic (composed of the Griesbachian, Dinerian, Smithian, and Spathian substages, respectively) in its entirety, although the isotopic profile is not continuous. By studying strata from northern Gondwana, now located on the northern margin of the Indian subcontinent in Pakistan, Indian Kashmir, Spiti (India) and Nepal (Fig. 1), it became apparent that the Early Triassic as a whole was isotopically anomalous [1,2,5]. At Nammal Gorge in the Salt Ranges (Pakistan), the $\delta^{13}C$ record is characterized by a return to mildly positive $\delta^{13}C$ values above the 'pre-boundary excursion' followed by a mildly negative $\delta^{13}C$ excursion through Upper Griesbachian strata. A minor positive trend is noted at the Griesbachian–Dienerian boundary, followed by a negative excursion that culminates in Middle Dienerian beds. Carbon isotope values return positive for the remaining Dienerian stage and culminate in a strong positive $\delta^{13}C$ excursion best recorded in the Losar section (Spiti, India) at or near

the Dienerian–Smithian boundary. Smithian strata return to mildly negative $\delta^{13}C$ values. A second strongly positive excursion occurs across the Smithian–Spathian boundary; it is pronounced at the Landu Nala section (–2 to +4‰), and even more pronounced in the Losar section (+5‰, Spiti, India). Lower Spathian strata record a final mildly negative $\delta^{13}C$ excursion, followed by a third pronounced positive excursion across the Spathian–Anisian boundary. Thus, the $\delta^{13}C$ record oscillates by at least 10‰ during the Early Triassic, as demonstrated by the northern Gondwana sections. In sum, the upper Lower Triassic $\delta^{13}C$ record is punctuated by three extraordinarily large positive shifts that correlate well with the recent results from China [80], discussed below. The $\delta^{13}C$ record from Oman (Batain region) reveals 10‰ $\delta^{13}C$ oscillations, as well [88].

The most recent dataset to date originates from the South China region [80], which represents an isolated carbonate platform on the far eastern margin of the Paleotethys during Early Triassic time (Fig. 2). The stratigraphic succession spans the Upper Permian, through the Middle Triassic, and into the Upper Triassic. The advantages of the South China section include relatively continuous carbonate platform sedimentation, the appropriate biostratigraphy, and the ability to compare pre- and post-Lower Triassic $\delta^{13}C$ profiles to the Lower Triassic profiles. Broadly, the results are strikingly similar to the Lower Triassic sections from the northern Indian subcontinent, but with greater sampling resolution. Notable differences are apparent during the Smithian-Spathian positive excursion: the Losar section, discussed above, reveals a more strongly positive excursion to $\delta^{13}C$ values than the South China sections. It should be noted that the biochronological calibration in the Losar section [1] is based on ammonoid biostratigraphy, whereas the South China section is based upon conodont biostratigraphy, and minor biostratigraphic offsets may be present. Regardless, the Lower Triassic succession from South China reveals remarkable $\delta^{13}C$ oscillations on the order of 10‰ over a 4- to 6-million-year period. Notably, the South China data reveal that the Middle Triassic $\delta^{13}C$ record is strikingly calm when compared to the Lower Triassic record.

3. Other isotopic records

The Early Triassic carbon isotopic record forms the core of this report, but new data from other isotopic systems have recently been available. For the Lower Triassic, trends in the $^{87}Sr/^{86}Sr$ ratio of seawater reveal a nearly monotonic rise from values near 0.7073 in the Latest Permian to an isotopic maximum of ~0.7083 immediately prior to the Lower–Middle Triassic boundary (Fig. 2) [34,58,59,70]. The cause of the rise is debated, but conventional interpretation would suggest that it results from an additional flux of radiogenic strontium via enhanced continental erosion or from a diminished hydrothermal input of non-radiogenic strontium to the oceans [49], or both. Because of the long residence time of strontium in the oceans, the detailed isotopic record facilitates substage correlation between successions locally and worldwide. Thus, the recently refined $^{87}Sr/^{86}Sr$ record will enhance the ability to correlate from place to place where faced with a depauperate Early Triassic fauna.

Until recently, sulfate minerals in evaporite facies provided the most reliable seawater proxy for $\delta^{34}S$. However, evaporites are temporally restricted and the construction of a continuous $\delta^{34}S$ record from evaporite provinces is not possible. For the Early Triassic, Holser et al. [41] provide a low-resolution compilation based on analyses from evaporite basins worldwide (Fig. 2) that reveals a remarkable 25‰ excursion from the Latest Permian (ca. +10‰) to a post-Cambrian maximum in the latest Early Triassic (ca. +35‰). The details of this trend over 4 to 6 Ma, however, are lacking, due to the paucity of evaporites through the interval of interest. Other evaporite-based data originate from the northern Calcareous Alps [92] and Abu Dhabi [105]. The profound sulfur isotopic shift must indicate highly unusual ocean chemistry, but no continuous isotopic profile has been produced to date. More recently, the $\delta^{34}S$ of sulfate bound in the calcium carbonate lattice from seawater at the time of deposition has been successfully analyzed [54,67,68,78]. Consequently, normal marine limestones allow the construction of relatively continuous $\delta^{34}S_{CAS}$ profiles, which are not possible with evaporite deposits. Significant $\delta^{34}S$ variations occur across the Permo-Triassic transition in the Italian Alps [78] and Turkey [68]. Uppermost Permian $\delta^{34}S$ values ~10‰ rise to values ~30‰ by the Mid-Griesbachian, thus verifying the anomalously enriched values identified by Holser et al. [41]. High amplitude changes are superimposed on this longer-term rise and appear to coincide with the end-Permian extinction level in the Italian sections. Marenco et al. [67] demonstrate

rapid δ^{34}S changes of nearly 20‰ over 100 m of stratigraphic section in Uppermost Spathian strata in the western United States and interpret such rapid isotopic change to indicate a depleted sulfate reservoir (cf. [51]). Like the carbon isotope record discussed above, a similar boundary-centric situation exists for the δ^{34}S record and additional data are needed for the remaining Early Triassic.

4. Discussion

4.1. What is responsible for the Early Triassic δ^{13}C record?

Hypotheses that explain the negative δ^{13}C anomaly in association with the Permian–Triassic transition fall into two categories: temporally instantaneous or temporally protracted. Unfortunately, the timing of the boundary δ^{13}C anomaly is unclear, as discussed above, and the radiometric calibration of the remaining Early Triassic is not available. It should be noted that most of the hypotheses discussed below were formulated before it was clear that the entire Early Triassic δ^{13}C record was so unusual and characterized by massive 10‰ changes. Thus, most workers likely assumed that the δ^{13}C record returned to 'normal' shortly after the boundary excursion. We now know this is not the case (Fig. 2), which clearly questions the validity of the instantaneous causes.

Instantaneous events include (1) the catastrophic release of methane from the gas hydrate reservoir with δ^{13}C ~–60‰, (2) the input of CO_2 from volcanic outgassing with δ^{13}C ~–6‰, and (3) the release of CO_2 from rotting terrestrial biomass after a catastrophic die-off with δ^{13}C ~–25‰. Many proponents of the methane source suggest the gas hydrate reservoir was destabilized by a bolide impact – for which there is little unambiguous evidence [26,48]. Modern estimates would suggest that the marine clathrate reservoir requires ~10 Myr to 'recharge' after a catastrophic release (e.g., [19]). Thus, if destabilization of clathrates caused the boundary excursion, alternate causes must be found to explain the Griesbachian, Smithian, and Spathian negative δ^{13}C excursions that followed, insofar as the entire Early Triassic may span only 4 to 6 Myr (cf. [56]). In addition, the shape of the isotopic profile for the post-boundary Early Triassic does not support a methane trigger. In general, clathrate destabilization is thought to produce an asymmetric δ^{13}C profile – cf. Paleocene–Eocene event [55] whereas the post-boundary profile is virtually symmetric going into and out of each δ^{13}C excursion – as noted by [80]. The Siberian Traps, a large magmatic province formed at the same time as the negative δ^{13}C anomaly (within radiometric error), is commonly cited as the prime volcanogenic culprit [84]. As with the gas hydrate model, it is unclear whether the Siberian Traps continued to erupt for the entire Early Triassic. On the other hand, the dating with respect to the upper limit of the volcanic flows is incomplete and the Siberian traps may remain a possible source of isotopically light carbon. The mass mortality followed by the mass rot-off is hypothesized to have occurred because of a bolide impact or other extraterrestrial cause; this instantaneous hypothesis suffers from the same deficiencies as the others. There is no evidence, for example, that the terrestrial biosphere was decimated and regenerated several times over the course of the Early Triassic.

Protracted causes for the δ^{13}C anomaly would include (1) ocean stratification/turnover and (2) the reorganization of the carbon cycle. The ocean stratification model would suggest that isotopically light organic matter produced in the photic zone would sink and become remineralized in the deeper portions of a stratified ocean, creating an isotopically heavy surface ocean and an isotopically depleted deep ocean. Carbonates deposited in surface waters during stratification would record isotopically heavy δ^{13}C values. The episodic overturn, or destratification, of such an ocean would return light carbon to the surface ocean and resulting in the negative δ^{13}C anomaly. Abundant evidence exists for anoxia during the Early Triassic, implying that a certain degree of stratification is likely [30,36,47,52,53,99–101,103]. Models of ocean circulation and chemistry, however, differ on whether or not whole ocean stratification is possible, and mass balance considerations are problematic (see below). The reorganization of the carbon cycle hypothesis involves the reduction in the burial flux of terrestrial biomass versus marine biomass. In this scenario, the reduction of the terrestrial biomass is shown by the noted 'coal gap' in the stratigraphic record and the change from high biomass arborescent plants in the Permian to low biomass herbaceous plants in the Early Triassic. Such a reorganization of the carbon cycle would change the burial proportion of terrestrial ver-

sus marine organic carbon and cause a long-term negative shift in the $\delta^{13}C$ of the oceans. Essentially, the burial of organic carbon would shift from terrestrial + marine to marine alone, causing the negative shift. This scenario is appealing for long-term changes in the carbon cycle, but is less appealing for rapid $\delta^{13}C$ shifts.

The negative $\delta^{13}C$ anomaly associated with the Permo-Triassic boundary has been modeled in an attempt to better understand the processes responsible for the $\delta^{13}C$ anomalies [10,14,31]. The models are restricted by the ambiguity surrounding the duration of the negative anomaly and similarly fall in to 'instantaneous' versus 'protracted' categories. Broecker and Peackock [14] modeled the reorganization of the carbon cycle, as outlined above. Their scenario fits both the $\delta^{13}C$ and the $\delta^{34}S$ record well, assuming that a long duration for the anomaly is chosen. Berner [10] assumes a short duration (~20 000) for the decline from positive to negative $\delta^{13}C$ values. Importantly, Berner's model demonstrated that the reservoir of isotopically depleted carbon available in the mass-mortality and overturn hypotheses was much too small to cause the observed $\delta^{13}C$ shift, regardless of the duration, and thus these hypotheses were rejected as sole causes. Even with such a short duration, methane release alone was not found to be sufficient to cause the boundary $\delta^{13}C$ anomaly, given reasonable rates of clathrate decomposition. Rather, the best model fit to the data occurred when multiple sources of isotopically depleted carbon were combined (cf. [24]). Such a combination of factors seems inevitable if we seek to explain the unusually variable Early Triassic $\delta^{13}C$ record. At any rate, the lack of consensus on the duration of the $\delta^{13}C$ boundary anomaly clouds such studies.

4.2. Early Cambrian versus Early Triassic $\delta^{13}C$ records

The Phanerozoic $\delta^{13}C$ record is somewhat tranquil with respect to multiple large and rapid swings in $\delta^{13}C$ when compared to the Early Triassic, although exceptions are clearly evident as high-resolution datasets are collected (e.g., [96]). The Early Cambrian, however, displays many of the same carbon isotopic features as the Early Triassic. As many as eight excursions are noted in Lower Cambrian strata over the course of approximately 20 Myr – see compilation in [57] – (Fig. 3); the magnitude of the excursions decreases from a maximum of ~10 ‰ at the Precambrian-Cambrian boundary to less than a few per mil at the Lower-Middle Cambrian boundary. It may not be wise to compare the two periods based solely on a perceived similarity in the magnitude and rapidity of their $\delta^{13}C$ records. However, comparative studies may reveal features not originally noted in one system or the other, so with caution, we will examine the similarities and differences between the Early Cambrian and Early Triassic biospheres.

Notable ecological confluences between the Early Cambrian and the Early Triassic set both periods apart from the remaining Phanerozoic. Similarities would include the importance (or lack thereof) of the terrestrial biosphere, the depth of infaunal tiering (e.g., [3]), and the average ichnofabric index [23]. The importance of a eukaryotic terrestrial biosphere as a carbon cycle moderator has been discussed above, and both the Cambrian and Triassic are characterized by a reduced terrestrial biosphere. The Ordovician and Silurian likely lacked a well-developed terrestrial biosphere, as well, but both record advanced ichnofabrics and relatively well-developed infaunal tiering [3,12]. In contrast, the Early Cambrian and the Early Triassic share a reduced average ichnofabric index and similarly reduced maximum depth of infaunal tiering [12]. The consequences of reduced sediment churning/oxygenation via bioturbation/infaunalization could

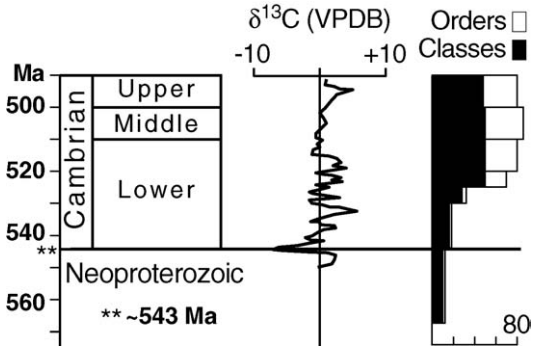

Fig. 3. Summary of the Cambrian $\delta^{13}C$ record (modified from [57]). Compare the variability in the Early Cambrian $\delta^{13}C$ record to Fig. 1 for the Early Triassic. Both time periods share reduced faunal tiering and overall ichnofabric index.

Fig. 3. Synthèse des valeurs du $\delta^{13}C$ du Cambrien (modifié d'après [57]). Comparer la variabilité des valeurs du $\delta^{13}C$ du Cambrien inférieur avec celle de la Fig. 1 concernant le Trias inférieur. Les deux intervalles de temps montrent une réduction comparable de l'importance de l'étagement de l'endofaune et, plus généralement, de l'indice textural de l'ichnofaune.

include a change in the way carbon is stored and recycled on the continental shelves. The bulk of modern organic carbon is buried in continental shelf environments. Perhaps a reduction in the biogenic sediment churning would enhance organic carbon burial, and thus drive the $\delta^{13}C$ of seawater to much heavier values, as noted in the Dienerian-Smithian boundary [80]. Such an enhanced organic carbon reservoir would return isotopically light carbon to the system if exhumed. These processes would clearly operate on longer time scales, consistent with the current $\delta^{13}C$ record for the Early Triassic, and would be enhanced by the presence of anoxic bottom waters.

5. Conclusion

The most recent $\delta^{13}C$ data indicate that the carbon cycle was unusual *throughout* Early Triassic time and that the 'boundary $\delta^{13}C$ excursion' near the Permian–Triassic transition simply marks the onset of 4 to 6 Myr of extraordinary changes in the $\delta^{13}C$ of seawater. Previous work had focused on the negative $\delta^{13}C$ excursion coincident with the final extinction in the Latest Permian with the tacit assumption that the carbon cycle returned to 'normal' following the boundary. Thus, hypotheses proposed to explain the boundary $\delta^{13}C$ phenomena did so without the knowledge that the carbon cycle remained perturbed for an additional 4 to 6 Myr. Therefore, causative processes with short or catastrophic origins that seemed reasonable at the time are currently viewed with more skepticism. It is notable that similarly large $\delta^{13}C$ fluctuations characterize both Early Triassic and Early Cambrian time. Other similarities would include a reduced terrestrial biosphere, a reduced depth of infaunal tiering, and a reduced ichnofabric index. Such factors may conspire to change the way organic carbon is stored and thus affect the $\delta^{13}C$ value of coeval seawater.

Acknowledgments

AB and SR are grateful to the Swiss National Foundation (projects No. 20-53787.98 and N°67941.02) and to the Geological Museum in Lausanne. FC and PM would like to than D. Bottjer, S. Pruss, M. Fraiser, A. J. Kaufman, and J. Payne for valuable discussions.

References

[1] N.-V. Atudorei, Constraints on the Upper Permian to Upper Triassic marine carbon isotope curve. Case studies from the Tethys, PhD thesis, Lausanne, Switzerland, 1999.

[2] V. Atudorei, A. Baud, Carbon isotope events during the Triassic, Albertiana 20 (1997) 45–49.

[3] W.I. Ausich, D.J. Bottjer, Tiering in suspension-feeding communities on soft substrata throughout the Phanerozoic, Science 216 (1982) 173–174.

[4] A. Baud, M. Magaritz, W.T. Holser, Permian–Triassic of the Tethys; Carbon isotope studies, Geol. Rundsch. 78 (1989) 649–677.

[5] A. Baud, V. Atudorei, Z. Sharp, Late Permian and Early Triassic evolution of the northern Indian margin; carbon isotope and sequence stratigraphy, Geodin. Acta 9 (1996) 57–77.

[6] A. Baud, V.-N. Atudorei, J. Marcoux, The Permian–Triassic boundary interval (PTBI) in Oman: Carbon isotope and facies changes, in: International Conference on Pangea and the Paleozoic-Mesozoic Transition, China University of Geosciences Press, Wuhan (China), 1999, pp. 88–89.

[7] A. Baud, S. Richoz, J. Marcoux, Calcimicrobial cap rocks from the basal Triassic units of the Taurus (SW Turkey), an anachronistic facies before the biotic recovery, C. R. Palevol 4, 2005 (this volume).

[8] B. Beauchamp, A. Baud, Growth and demise of Permian biogenic chert along Northwest Pangea; evidence for end-Permian collapse of thermohaline circulation, Paleogeogr., Paleoclimatol., Paleoecol. 184 (2002) 37–63.

[9] L. Becker, R.J. Poreda, A.G. Hunt, T.E. Bunch, M. Rampino, Impact event at the Permian–Triassic boundary; evidence from extraterrestrial noble gases in fullerenes, Science 291 (2001) 1530–1533.

[10] R.A. Berner, Examination of hypotheses for the Permo-Triassic boundary extinction by carbon cycle modeling, Proc. Natl Acad. Sci. USA 99 (2002) 4172–4177.

[11] H. Bosscher, W. Schlager, Accumulation rates of carbonate platforms, J. Geol. 101 (1993) 345–355.

[12] D.J. Bottjer, W.I. Ausich, Phanerozoic development of tiering in soft substrata suspension-feeding communities, Paleobiology 12 (1986) 400–420.

[13] S.A. Bowring, D.H. Erwin, Y.G. Jin, M.W. Martin, K. Davidek, W. Wang, U/Pb zircon geochronology and tempo of the end-Permian mass extinction, Science 280 (1998) 1039–1045.

[14] W.S. Broecker, S. Peacock, An ecological explanation for the Permo-Triassic carbon and sulfur isotope shifts, Global Biogeochem. Cycles 13 (1999) 1167–1172.

[15] R. Buick, J.A. Nicol, L. Watson, D.C. Catling, Multiple carbon isotope excursions at the Permian–Triassic boundary separating two mass extinctions, in: Second Astrobiology Science Conference, NASA Ames Research Center, NASA, 2002.

[16] J. Chen, M. Shao, W. Huo, Y. Yao, Carbon isotope of carbonate strata at Permian–Triassic boundary in Changxing, Zhejiang, Acta Geol. Sin. 1984 (1984) 88–93.

[17] L. Clemmensen, W.T. Holser, D. Winter, Stable isotope study through the Permian–Triassic boundary in East Greenland, Bull. Geol. Soc. Denmark 33 (1985) 253–260.

[18] M.J. de Wit, J.G. Ghosh, S. de Villiers, N. Rakotosolofo, J. Alexander, A. Tripathi, C. Looy, Multiple organic carbon isotope reversals across the Permo-Triassic boundary of terrestrial Gondwana sequences; clues to extinction patterns and delayed ecosystem recovery, J. Geol. 110 (2002) 227–246.

[19] G.R. Dickens, Rethinking the global carbon cycle with a large, dynamic and microbially mediated gas hydrate capacitor, Earth Planet. Sci. Lett. 213 (2003) 169–182.

[20] T. Dolenec, S. Buser, M. Dolenec, The Permian–Triassic Boundary in the Karawanke Mountains (Slovenia): stable isotope variations in the boundary carbonate rocks of the Kosutnik Creek and Brsnina section, Geologija i Geofizika 41 (1998) 17–27.

[21] T. Dolenec, S. Lojen, M. Dolenec, The Permian–Triassic Boundary in the Idrijca Valley (Western Slovenia): isotopic fractionation between carbonate and organic carbon at the P/Tr transition, Geologija i Geofizika 42 (1999) 165–170.

[22] T. Dolenec, S. Lojen, A. Ramovs, The Permian–Triassic boundary in western Slovenia (Idrijca Valley section); magnetostratigraphy, stable isotopes, and elemental variations, Chem. Geol. 175 (2001) 175–190.

[23] M.L. Droser, D.J. Bottjer, Trends in depth and extent of bioturbation in Cambrian carbonate marine environments, western United States, Geology 16 (1988) 233–236.

[24] D.H. Erwin, The Great Paleozoic Crisis: Life and Death in the Permian, Columbia University Press, New York, 1993, 327 p.

[25] D.H. Erwin, S.A. Bowring, Y. Jin, End-Permian mass extinctions; a review, in: C. Koeberl, K.G. MacLeod (Eds.), Catastrophic events and mass extinctions; impacts and beyond-GSA, Special Paper 356, Geological Society of America, Boulder, 2002, pp. 363–383.

[26] K.A. Farley, Mukhopadhyay, An extraterrestrial impact at the Permian–Triassic boundary?, Science 293 (2001) 2343.

[27] K. Faure, M.J. de Wit, J.P. Willis, Late Permian global coal hiatus linked to ^{13}C-depleted CO_2 flux into the atmosphere during the final consolidation of Pangea, Geology 23 (1995) 507–510.

[28] C.B. Foster, G.A. Logan, R.E. Summons, The Permian–Triassic boundary in Australia – Organic carbon isotopic anomalies relate to organofacies, not a biogeochemical 'event', in: Ninth Annual Goldschmidt Conference, Cambridge MA, USA, 1999, pp. 110.

[29] C.B. Foster, G.A. Logan, R.E. Summons, J.D. Gorter, D.S. Edwards, in: Carbon isotopes, kerogen types and the Permian–Triassic boundary in Australia: implications for exploration, APPEA J, 1997, pp. 472–489.

[30] P. Ghosh, S.K. Bhattacharya, A.D. Shukla, P.N. Shukla, N. Bhandari, G. Parthasarathy, A.C. Kunwar, Negative $\delta^{13}C$ excursion and anoxia at the Permo-Triassic boundary in the Tethys Sea, Curr. Sci. 83 (2002) 498–502.

[31] A. Grard, L.M. François, C. Dessert, B. Dupré, Y. Goddéris, Basaltic volcanism and mass extinction at the Permo-Triassic boundary: Environmental impact and modeling of the global carbon cycle, Earth Planet. Sci. Lett. 234 (2005) 207–221.

[32] K. Grice, R. Twitchett, C. Foster, R.E. Summons, E. Grosjean, E. Krull, C. Barber, R. Alexander, P. Greenwood, G.A. Logan, Biomarker distributions and their stable isotopes in marine Permian/Triassic sections from around the globe; searching for clues to the cause of the end-Permian mass extinction event, in: Australian Organic Geochemistry Conference, CSIRO, North Ryde, N.S.W., 2004.

[33] M. Gruszczynski, S. Halas, A. Hoffman, K. Malkowski, A brachiopod calcite record of the oceanic carbon and oxygen isotope shifts at the Permian/Triassic transition, Nature 337 (1989) 64–68.

[34] M. Gruszczynski, A. Hoffman, K. Malkowski, J. Veizer, Seawater strontium isotopic perturbation at the Permian–Triassic boundary, West Spitsbergen, and its implications for the interpretation of strontium isotopic data, Geology 20 (1992) 779–782.

[35] A. Hallam, Why was there a delayed radiation after the end-Paleozoic extinctions?, in: M. Brasier (Ed.), Innovations and revolution in the biosphere 5, Harwood Academic Publishers, 1991, pp. 257–262.

[36] A. Hallam, The Earliest Triassic as an anoxic event, and its relationship to the end-Paleozoic mass extinction, in: A.F. Embry, B. Beauchamp, D.J. Glass (Eds.), Pangea conference 17, Canadian Society of Petroleum Geologists, 1994, pp. 797–804.

[37] A. Hallam, P.B. Wignall, Mass extinctions and their aftermath, Oxford University Press, New York, 1997, 320 p.

[38] H.J. Hansen, S. Lojen, P. Toft, T. Dolenec, J. Tong, P. Michaelsen, A. Sarkar, Magnetic susceptibility and organic carbon isotopes of sediments across some marine and terrestrial Permo-Triassic boundaries, in: H. Yin, J.M. Dickins, G.R. Shi, J. Tong (Eds.), Permian–Triassic evolution of Tethys and western Circum-Pacific, Developments in Paleontology and Stratigraphy 18, Elsevier, Amsterdam, The Netherlands, 2000, pp. 271–289.

[39] E. Heydari, J. Hassanzadeh, W.J. Wade, Geochemistry of central Tethyan Upper Permian and Lower Triassic strata, Abadeh region, Iran, Sediment. Geol. 137 (2000) 85–99.

[40] W.T. Holser, M. Magaritz, The Late Permian carbon isotope anomaly in the Bellerophon Basin, Carnic and Dolomite Alps, Jahrb. Geol. Bundesanst. Wien 128 (1985) 75–82.

[41] W.T. Holser, M. Magaritz, Events near the Permian–Triassic boundary, Modern Geol. 11 (1987) 155–180.

[42] W.T. Holser, H.-P. Schoenlaub, M. Attrep Jr., K. Boeckelmann, P. Klein, M. Magaritz, C.J. Orth, A. Fenninger, C. Jenny, M. Kralik, H. Mauritsch, E. Pak, J.-M. Schramm, K. Stattegger, R. Schmoeller, A unique geochemical record at the Permian/Triassic boundary, Nature 337 (1989) 39–44.

[43] W.T. Holser, H.-P. Schönlaub, K. Boeckelman, M. Magaritz, The Permian–Triassic of the Gartnerkofel-1 core (Carnic Alps, Austria): Synthesis and conclusions, in: W.T. Holser, H.P. Schönlaub (Eds.), The Permian–Triassic boundary in the Carnic Alps of Austria (Gartnerkofel Region), Abh. Geol. Bundesanst. Wien 45, 1991, pp. 213–232.

[44] M. Horacek, R. Brandner, R. Abart, A positive $\delta^{13}C$ excursion recorded by Lower Triassic marine carbonates from the western central Dolomites, N.-Italy, a special situation in the western Tethys?, in: 31st International Geological Congress, Rio de Janeiro, IGC, 2000.

[45] R.M. Hotinski, K.L. Bice, L.R. Kump, R.G. Najjar, M.A. Arthur, Ocean stagnation and end-Permian anoxia, Geology 29 (2001) 7–10.

[46] H. Ishiga, K. Ishida, Y. Sampei, M. Musashino, S. Yamakita, Y. Kajiwara, T. Morikiyo, Oceanic pollution at the Permian–Triassic boundary in pelagic condition from carbon and sulfur stable isotopic excursion, Southwest Japan, Bull. Geol. Surv. Jpn 44 (1993) 721–726.

[47] Y. Isozaki, Permo-Triassic boundary superanoxia and stratified superocean; records from lost deep sea, Science 276 (1997) 235–238.

[48] Y. Isozaki, An extraterrestrial impact at the Permian–Triassic boundary?, Science 293 (2001) 2343.

[49] S.B. Jacobsen, A.J. Kaufman, The Sr, C and O isotopic evolution of Neoproterozoic seawater, Geochim. Cosmochim. Acta 161 (1999) 37–57.

[50] Y.G. Jin, Y. Wang, W. Wang, Q.H. Shang, C.Q. Cao, D.H. Erwin, Pattern of marine mass extinction near the Permian–Triassic boundary in South China, Science 289 (2000) 432–436.

[51] L.C. Kah, T.D. Frank, T.W. Lyons, Low marine sulphate and protracted oxygenation of the Proterozoic biosphere, Nature 431 (2004) 834–838.

[52] K. Kaiho, Y. Kajiwara, T. Nakano, Y. Miura, H. Kawahata, K. Tazaki, M. Ueshima, Z. Chen, G.R. Shi, End-Permian catastrophe by a bolide impact; evidence of a gigantic release of sulfur from the mantle, Geology 29 (2001) 815–818.

[53] Y. Kajiwara, S. Yamakita, K. Ishida, H. Ishiga, A. Imai, Development of a largely anoxic stratified ocean and its temporary massive mixing at the Permian/Triassic boundary supported by the sulfur isotopic record, Paleogeogr., Paleoclimatol., Paleoecol. 111 (1994) 367–379.

[54] A. Kampschulte, H. Strauss, The sulfur isotopic evolution of Phanerozoic seawater based on the analysis of structurally substituted sulphate in carbonates, Chem. Geol. 204 (2004) 255–286.

[55] J.P. Kennett, L.D. Stott, Abrupt deep-sea warming, paleoceanographic changes and benthic extinctions at the end of the Paleocene, Nature 353 (1991) 225–229.

[56] J.P. Kennett, K.G. Cannariato, I.L. Hendy, R.J. Behl, Carbon isotopic evidence for methane hydrate instability during Quaternary interstadials, Science 288 (2000) 128–133.

[57] A.H. Knoll, S.B. Carroll, Early animal evolution; emerging views from comparative biology and geology, Science 284 (1999) 2129–2137.

[58] C. Korte, (Ed), $^{87}Sr/^{86}Sr$, $\delta^{18}O$, und $\delta^{13}C$-Evolution des triassischen Meerwassers: Geochemische und stratigraphische Untersuchungen an Conodonten und Brachiopoden, in: Bochum University, Bochum, Germany, 1999, 172 p.

[59] C. Korte, H.W. Kozur, P. Bruckschen, J. Veizer, Strontium isotope evolution of Late Permian and Triassic seawater, Geochim. Cosmochim. Acta 67 (2003) 47–62.

[60] C. Korte, H.W. Kozur, M. Joachimski, H. Strauss, J. Veizer, L. Schwark, Carbon, sulfur, oxygen and strontium isotope records, organic geochemistry and biostratigraphy across the Permian/Triassic boundary in Abadeh, Iran, Int. J. Earth Sci. 93 (2004) 565–581.

[61] E.S. Krull, G.J. Retallack, H.J. Campbell, G.L. Lyon, $\delta^{13}C_{org}$ chemostratigraphy of the Permian–Triassic boundary in the Maitai Group, New Zealand: evidence for high-latitudinal methane release, N. Z. J. Geol. Geophys. 43 (2000) 21–32.

[62] E.S. Krull, D.J.D.D. Lehrmann, B.Y.Y. Kessel, R. Li, Stable carbon isotope stratigraphy across the Permian–Triassic boundary in shallow marine carbonate platforms, Nanpanjiang Basin, South China, Paleogeogr., Paleoclimatol., Paleoecol. 204 (2004) 297–315.

[63] L. Krystyn, S.B.A. Richoz, R.J. Twitchett, A. Baud, A unique Permian–Triassic boundary section from the Neotethyan Hawasina Basin, central Oman Mountains, in: A. Baud, B. Beauchamp, J. Marcoux, R.J. Twitchett (Eds.), International conference on the Geology of Oman, Pangea Symposium Paleogeogr., Paleoclimatol., Paleoecol.191, Elsevier, 2003, pp. 329–344.

[64] M. Magaritz, ^{13}C minima follow extinction events; a clue to faunal radiation, Geology 17 (1989) 337–340.

[65] M. Magaritz, R. Baer, A. Baud, W.T. Holser, The carbon-isotope shift at the Permian/Triassic boundary in the southern Alps is gradual, Nature 331 (1988) 337–339.

[66] K. Malkowski, M. Gruszczynski, A. Hoffman, S. Halas, Oceanic stable isotope composition and a scenario for the Permo-Triassic crisis, Hist. Biol. 2 (1989) 289–309.

[67] P.J. Marenco, F.A. Corsetti, D.J. Bottjer, Chemostratigraphy of the Union Wash Formation: Implications for the Early Triassic recovery from the Permian Triassic mass extinction, in: Geological Society of America Annual Meeting Abstracts, vol. 34, 2002, 508 p.

[68] P.J. Marenco, A. Baud, F.A. Corsetti, D.J. Bottjer, A.J. Kaufman, Sulfur isotope anomalies across Permo-Triassic boundary sections in Turkey, in: Geological Society of America Annual Meeting Abstracts, vol. 36, 2004, 335 p.

[69] C.R. Marshall, Confidence intervals on stratigraphic ranges with nonrandom distributions of fossil horizons, Paleobiology 23 (1997) 165–173.

[70] E.E. Martin, J.D. Macdougall, Sr and Nd isotopes at the Permian/Triassic boundary: A record of climate change, Chem. Geol. 125 (1995) 73–99.

[71] M.W. Martin, D.J. Lehrman, S.A. Bowring, P. Enos, J. Ramezani, J. Wei, J. Zhang, Timing of the Lower Triassic carbonate bank buildup and biotic recovery following the end-Permian mass extinction across the Nanpanjiang Basin, South China, in: Geological Society of America Annual Meeting Abstracts, vol. 33, 2001, 201 p.

[72] R.E. Martin, G.J. Vermeij, D. Dorritie, K. Caldeira, M.R. Rampino, A.H. Knoll, R.K. Bambach, D. Canfield, J.P. Grotzinger, P.B. Wignall, R.J. Twitchett, Late Permian extinctions; discussion and reply, Science 274 (1996) 1549–1552.

[73] R. Morante, Carbon isotope stratigraphy of the Permian–Triassic in Australian marine and nonmarine sedimentary basins, in: Final meeting of IGCP Project 293 on Geochemical event markers in the Phanerozoic, Erlangen, Germany, 26–28 September 1994, 122, 1994, 43 p.

[74] R. Morante, Permian and Early Triassic isotopic records of carbon and strontium in Australia and a scenario of events about the Permian–Triassic boundary, Hist. Biol. 11 (1996) 289–310.

[75] R. Mundil, K.R. Ludwig, I. Metcalfe, P.R. Renne, Age and timing of the Permian mass extinctions: U/Pb dating of closed-system zircons, Science 305 (2004) 1760–1763.

[76] M. Musashi, Y. Isozaki, T. Koike, R. Kreulen, Stable carbon isotope signature in mid-Panthalassa shallow-water carbonates across the Permo-Triassic boundary: evidence for ^{13}C-depleted superocean, Earth Planet. Sci. Lett. 191 (2001) 9–20.

[77] J. Nan, D. Zhou, J. Ye, Z. Wang, Geochemistry of the paleoclimate and paleo-ocean environment during the Permian–Triassic in Guizhou, China, Acta Mineral. Sin. 18 (1998) 239–249.

[78] R. Newton, P. Pevitt, P.B. Wignall, S. Bottrell, Large shifts in the isotopic composition of seawater sulphate across the Permo-Triassic boundary in northern Italy, Earth Planet. Sci. Lett. 218 (2004) 331–345.

[79] H. Oberhansli, K.J. Hsu, S. Piasecki, H. Weissert, Permian–Triassic carbon-isotope anomaly in Greenland and in the Southern Alps, Hist. Biol. 2 (1989) 37–49.

[80] J.L. Payne, D.J. Lehrmann, J. Wei, M.J. Orchard, D.P. Schrag, A.H. Knoll, Large perturbations of the carbon cycle during recovery from the end-Permian extinction, Science 305 (2004) 506–509.

[81] S.B. Pruss, D.J. Bottjer, Late Early Triassic microbial reefs of the western United States: a description and model for their deposition in the aftermath of the end-Permian mass extinction, Paleogeogr., Paleoclimatol., Paleoecol. 211 (2004) 127–137.

[82] M.R. Rampino, A. Prokoph, A. Adler, Tempo of the end-Permian event; high-resolution cyclostratigraphy at the Permian–Triassic boundary, Geology 28 (2000) 643–646.

[83] D.M. Raup, Size of the Permo-Triassic bottleneck and its evolutionary implications, Science 206 (1979) 217–218.

[84] P.R. Renne, Z. Zhang, M.A. Richards, M.T. Black, A.R. Basu, Synchrony and causal relations between Permian–Triassic boundary crises and Siberian flood volcanism, Science 269 (1995) 1413–1416.

[85] G.J. Retallack, Postapocalyptic greenhouse paleoclimate revealed by Earliest Triassic paleosols in the Sydney Basin, Australia, Geol. Soc. Am. Bull. 111 (1999) 52–70.

[86] G.J. Retallack, J.J. Veevers, R. Morante, Global coal gap between Permian–Triassic extinction and Middle Triassic recovery of peat-forming plants, Geol. Soc. Am. Bull. 108 (1996) 195–207.

[87] G.J. Retallack, W.T. Holser, Y. Isozaki, Timing of Permian–Triassic anoxia; discussion and reply, Science 277 (1997) 1748–1749.

[88] S. Richoz, Stratigraphie et variations isotopiques du carbone dans le Permien supérieur et le Trias inférieur de la Néotéthys (Turquie, Oman et Iran), PhD thesis, Lausanne, Switzerland, 2004.

[89] A. Sarkar, H. Yoshioka, M. Ebihara, H. Naraoka, Geochemical and organic carbon isotope studies across the continental Permo-Triassic boundary of Raniganj Basin, eastern India, Paleogeogr., Paleoclimatol., Paleoecol. 191 (2003) 1–14.

[90] V. Schwab, J.E. Spangenberg, Organic geochemistry across the Permian–Triassic transition at the Idrijca Valley, Western Slovenia, Appl. Geochem. 19 (2004) 55–72.

[91] M.A. Sephton, C.V. Looy, R.J. Veefkind, H. Brinkhuis, L.J.W.d.H. Visscher, Synchronous record of $\delta^{13}C$ shifts in the oceans and atmosphere at the end of the Permian, in: C. Koeberl, G. MacLeod Kenneth (Eds.), Catastrophic events and mass extinctions; impacts and beyond., GSA Special Paper 356, Geological Society of America, Boulder, CO, USA, 2002, pp. 455–462.

[92] C. Spötl, E. Pak, A strontium and sulfur isotopic study of Permo-Triassic evaporites in the Northern Calcareous Alps, Austria, Chem. Geol. 131 (1996) 219–234.

[93] S.M. Stanley, X. Yang, A double mass extinction at the end of the Paleozoic Era, Science 266 (1994) 1340–1344.

[94] L. Stemmerik, S. Piasezki, Carbon isotope shifts accross the Permian–Triassic boundary in East Greenland, in: Sedimentary events and Hydrocarbon systems, CSPG–SEPM, Calgary, Alberta, Canada, 1997, 264 p.

[95] R.J. Twitchett, C.V. Looy, R. Morante, H. Visscher, P.B. Wignall, Rapid and synchronous collapse of marine and terrestrial ecosystems during the end-Permian biotic crisis, Geology 29 (2001) 351–354.

[96] J. Veizer, D. Ala, K. Azmy, P. Bruckschen, D. Buhl, F. Bruhn, G.A.F. Carden, A. Diener, S. Ebneth, Y. Godderis, T. Jasper, C. Korte, F. Pawellek, O.G. Podlaha, H. Strauss, $^{87}Sr/^{86}Sr$, $\delta^{13}C$ and $\delta^{18}O$ evolution of Phanerozoic seawater, Chem. Geol. 161 (1999) 59–88.

[97] K. Wang, H.H.J. Geldsetzer, H.R. Krouse, Permian–Triassic extinction; organic $\delta^{13}C$ evidence from British Columbia, Canada, Geology 22 (1994) 580–584.

[98] K. Wang, W.D. Goodfellow, M.Q. Wu, H.R. Krouse, Organic carbon isotope variations in three leading candidate sections for the Permian–Triassic boundary global stratotype (Meishan, Shangsi and Huangsi, South China), in: 30th IGC Conference Abstracts, Beijing, 1996, 59 p.

[99] P.B. Wignall, A. Hallam, Anoxia as a cause of the Permian/Triassic mass extinction; facies evidence from northern Italy and the Western United States, Paleogeogr., Paleoclimatol., Paleoecol. 93 (1992) 21–46.

[100] P.B. Wignall, A. Hallam, Griesbachian (Earliest Triassic) paleoenvironmental changes in the Salt Range, Pakistan and Southeast China and their bearing on the Permo-Triassic mass extinction, Paleogeogr., Paleoclimatol., Paleoecol. 102 (1993) 215–237.

[101] P.B. Wignall, R.J. Twitchett, Oceanic anoxia and the end Permian mass extinction, Science 272 (1996) 1155–1158.

[102] P.B. Wignall, R. Morante, R. Newton, The Permo-Triassic transition in Spitsbergen; $\delta^{13}C_{org}$ chemostratigraphy, Fe and S geochemistry, facies, fauna and trace fossils, Geol. Mag. 135 (1998) 47–62.

[103] A.D. Woods, D.J. Bottjer, Distribution of ammonoids in the Lower Triassic Union Wash Formation (eastern California); evidence for paleoceanographic conditions during recovery from the end-Permian mass extinction, Palaios 15 (2000) 535–545.

[104] A.D. Woods, D.J. Bottjer, M. Mutti, J. Morrison, Lower Triassic large sea-floor carbonate cements; their origin and a mechanism for the prolonged biotic recovery from the end-Permian mass extinction, Geology 27 (1999) 645–648.

[105] R.H. Worden, P.C. Smalley, A.E. Fallick, Sulfur cycle in buried evaporites, Geology 25 (1997) 643–646.

[106] D.-Y. Xu, Z. Yan, Carbon isotope and iridium event markers near the Permian/Triassic boundary in the Meishan section, Zhejiang Province, China, in: H.H.J. Geldsetzer, G.S. Nowlan (Eds.), Joint Meeting of IGCP projects 216, 293, and 303 104, Elsevier, 1993, pp. 171–175.

[107] H. Yin, K. Zhang, J. Tong, Z. Yang, S. Wu, The Global Stratotype Section and Point (GSSP) of the Permian–Triassic boundary, Episodes 24 (2001) 102–114.

[108] Y.D. Zakharov, N.G. Ukhaneva, A.V. Ignatyev, T.V. Afanasyeva, G.I. Buryi, E.S. Panasenko, A.M. Popov, T.A. Punina, A.K. Cherbadzhi, Latest Permian and Triassic carbonates of Russia; stable isotopes, Ca–Mg ratio, and correlation, in: H. Yin, J. Tong (Eds.), Int. Conf. on Pangea and the Paleozoic–Mesozoic transition, China University of Geosciences Press, Wuhan, China, 1999.

[109] R. Zhang, M.J. Follows, J.P. Grotzinger, J. Marshall, Could the Late Permian deep ocean have been anoxic?, Paleoceanography 16 (2001) 317–329.